Chemical Science

EDGE ARTICLE

View Article Online
View Journal | View Issue

Cite this: *Chem. Sci.*, 2018, **9**, 1860

Diselenolane-mediated cellular uptake†

Nicolas Chuard,[a] Amalia I. Poblador-Bahamonde,[a] Lili Zong,[a] Eline Bartolami,[a] Jana Hildebrandt,[b] Wolfgang Weigand,[b] Naomi Sakai[a] and Stefan Matile *[a]

Received 4th December 2017
Accepted 2nd January 2018

DOI: 10.1039/c7sc05151d

rsc.li/chemical-science

The emerging power of thiol-mediated uptake with strained disulfides called for a move from sulfur to selenium. We report that according to results with fluorescent model substrates, cellular uptake with 1,2-diselenolanes exceeds uptake with 1,2-dithiolanes and epidithiodiketopiperazines with regard to efficiency as well as intracellular localization. The diselenide analog of lipoic acid performs best. This 1,2-diselenolane delivers fluorophores efficiently to the cytosol of HeLa Kyoto cells, without detectable endosomal capture as with 1,2-dithiolanes or dominant escape into the nucleus as with epidithiodiketopiperazines. Diselenolane-mediated cytosolic delivery is non-toxic (MTT assay), sensitive to temperature but insensitive to inhibitors of endocytosis (chlorpromazine, methyl-β-cyclodextrin, wortmannin, cytochalasin B) and conventional thiol-mediated uptake (Ellman's reagent), and to serum. Selenophilicity, the extreme CSeSeC dihedral angle of 0° and the high but different acidity of primary and secondary selenols might all contribute to uptake. Thiol-exchange affinity chromatography is introduced as operational mimic of thiol-mediated uptake that provides, in combination with rate enhancement of DTT oxidation, direct experimental evidence for existence and nature of the involved selenosulfides.

Unlike simple alkanes or peroxides, the most favorable CXXC dihedral angle θ in acyclic diselenides **1** and disulfides **2** is ~90° (X = S, Se, Fig. 1).[1] Decreasing θ in cyclic disulfides causes the increase of ring tension in 1,2-dithianes with 62° over 1,2-dithiolanes **3–4** with 27–35° to approach the maximum epidithiodiketopiperazine (ETP) **5** with ~0°.[2] Earlier, we found the dependence of the ability of cyclic disulfides as delivery vehicles of otherwise cell-impermeable cargos to the ring tension.[1,2] Mechanistic studies support that the ring tension promotes dynamic covalent thiol-disulfide exchange on the cell surface[1–6] to initiate uptake.[1,2] Asparagusic acid (SA) derivative **4** efficiently delivers functional peptides and objects as large as intact liposomes.[6]

This emerging power of strain-promoted thiol-mediated uptake with cyclic disulfides called for cyclic diselenides. Besides many similarities, disulfides and -selenides have also important differences. In six-membered rings, a very similar θ of ~60° (56°) has been confirmed.[7] In the crystal structure of 1,2-diselenolanes like SeA **6**, the CSeSeC dihedral angle is 0.2°, contributing to an almost ideal, twist-free envelope structure of the five-membered ring.[8,9] At the same time, the Se–Se bond

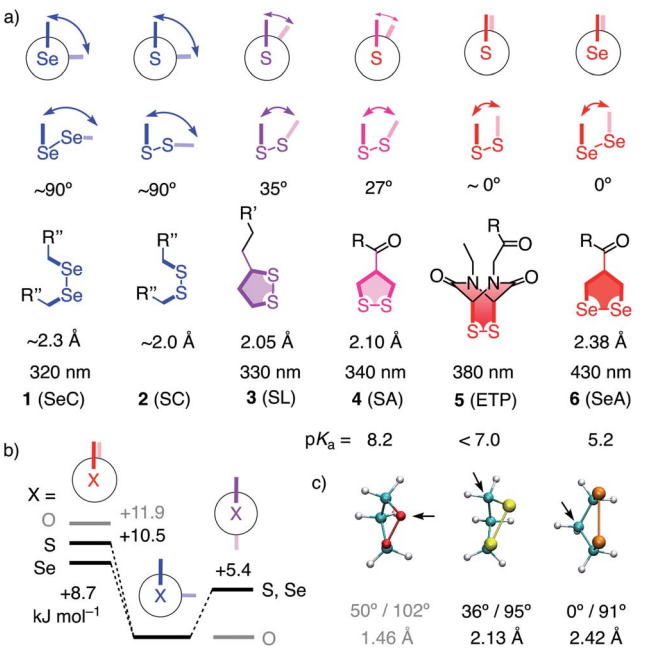

Fig. 1 (a) Selected CXXC dihedral angles, XX bond length and absorption maxima of disulfides and diselenides, and the intrinsic pK_a of one thiol or selenol in their reduced form (X = S, Se; R, R′, R″, see Fig. 2). (b) B3LYP/6-311++G** energies of MeXXMe conformers. (c) Minimized structure of the parent 1,2-dioxo- (O = red), dithio- (S = yellow) and diselenolane (Se = orange) with angles (CXXC, CXX) and bond length (XX), arrows: *endo* position.

[a]*Department of Organic Chemistry, University of Geneva, Geneva, Switzerland. E-mail: stefan.matile@unige.ch; Web: http://www.unige.ch/sciences/chiorg/matile/; Tel: +41 22 379 6523*

[b]*Institute of Inorganic and Analytical Chemistry, Friedrich-Schiller University Jena, Germany*

† Electronic supplementary information (ESI) available: Detailed procedures and results for all reported experiments. See DOI: 10.1039/c7sc05151d

length increases from ~2.3 Å in relaxed diselenides **1** to 2.38 Å in 1,2-diselenolane **6**, and the absorption maximum shifts 320 nm to 430 nm.[8–10] The CSSC dihedrals of 1,2-dithiolanes maximize at 27° in SAs such as **4**, and absorptions shift from 250 nm to maximal 340 nm.[1] The crystal structures of 1,2-di-selenolanes show layers of selenium with chalcogen bonds[11] of down to 3.55 Å length between the polarizable selenium atoms of different molecules.[8,9] In the solid state, the strained di-selenolanes easily polymerize into a gum.[9] In solution, relaxed diselenides exchange up to 7 orders of magnitude faster than disulfides.[12,13] The high acidity of selenols ($pK_a \sim 5.2$) compared to thiols ($pK_a \sim 8.2$) contributes to this increased reactivity by activating both nucleophile and leaving group for selenol–diselenide exchange in neutral and also slightly acidic water.[12–17] However, although exchange is possible with both thiols and selenols,[12] the formation of Se–Se bonds is favored over mixed S–Se bonds.[13] This selenophilicity has been used elegantly to catalyze protein folding[15] and protein denaturation with di-selenides in the presence of immobilized thiols.[16]

Some of the characteristics of 1,2-diselenolanes are reminiscent of ETPs **5** (*i.e.*, $pK_a < 7$, CXXC dihedral ~0°, Fig. 1) and could thus promise similarly outstanding uptake efficiencies with dual activation at highest tension.[2] Worthwhile to note in this context is also the presence of eight out of the 25 human selenoproteins in cellular membranes, which could potentially participate in selenol–diselenide exchange reactions during the uptake of diselenides.[17] Moreover, cellular uptake, particularly gene transfection, with tension-free poly(diselenide)s and poly(ditelluride)s has been reported to occur and differ sometimes favorably from uptake with poly(disulfide)s.[18] In the following, we report uptake of 1,2-diselenolanes SeL **7** and SeA **6** to the cytosol without endosomal capture as with the corresponding 1,2-dithiolanes SL **3** and SA **4** or dominant escape into the nucleus as with ETP **5**.

To elaborate on diselenolane-mediated uptake, green-fluorescent fluorescein isothiocyanate (FITC) conjugates were synthesized. SeL **7** was prepared from dichloride **8** (Fig. 2 and Scheme S1†). The reaction with Na_2Se_2 afforded the 1,2-di-selenolane scaffold as in the previously reported diseleno lipoic acid **9**.[19] Activation with *N*-hydroxysuccinimide (NHS) afforded the "SeL tag" **10**, an activated ester that reacted readily with amines such as FITC-amine **11** to afford SeL **7**. The green-fluorescent diselenolane SeA **6** was prepared from diseleno asparagusic acid[7,8] following the same route (Scheme S2†), and the acyclic diselenide **1** was obtained by reaction of methylated diseleno cystine (SeC)[20] with FITC (Scheme S3†). The control compounds SA **4** and ETP **5** were prepared following previously reported procedures.[1,2]

In computational studies, the minima at 90° and maxima at 0° in the conformational profiles of MeSeSeMe and MeSSMe were confirmed, whereas MeOOMe naturally minimized in *anti* conformation (Fig. 1b). The decreasing energy of the maxima from O to S and Se at 0° supported that ring tension in cyclic diselenides is lower than in disulfides. For unsubstituted 1,2-dioxo-, dithio- and diselenolanes, this trend resulted in envelope conformers with the chalcogen atom, the α carbon, and the β carbon in *endo* position and CXX angles decreasing from 102° to 95° and 91°, respectively (arrows, Fig. 1).

With tris(2-carboxyethyl)phosphine (TCEP), 1,2-diselenolane **9** was readily reduced to diselenol SeL^R **12′** (Fig. 2). However, neither SeA nor SeL appeared to react with various thiols **13** (Fig. 3). These results implied that either diselenides do not undergo exchange reactions with thiolates or, unlike S–S homologs **14**, the selenosulfide intermediate products **15–17** ring close easily by intramolecular selenol–selenosulfide exchange. Their existence and nature was thus explored by thiol-exchange affinity chromatography (Fig. 3). Compared to a non-reactive carboxyfluorescein (CF) standard (Fig. 3a), all disulfides and diselenides showed delayed elution as expected

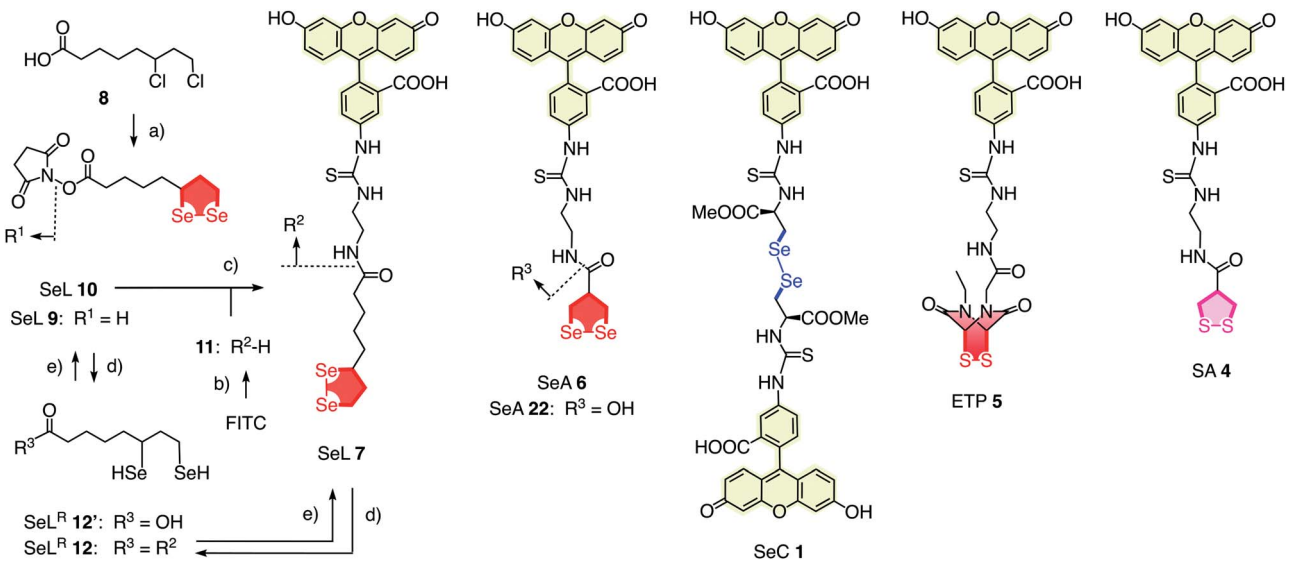

Fig. 2 Complete structure of all transporters used (neutral form), with representative synthesis and reduction for SeL **7**. (a) (1) Several steps, ref. 17, (2) NHS, DCC, THF, rt, 18 h, 53%; (b) several steps, ref. 1; (c) DMF, rt, 3 h, 14%; (d) TCEP, <5 min; (e) air.

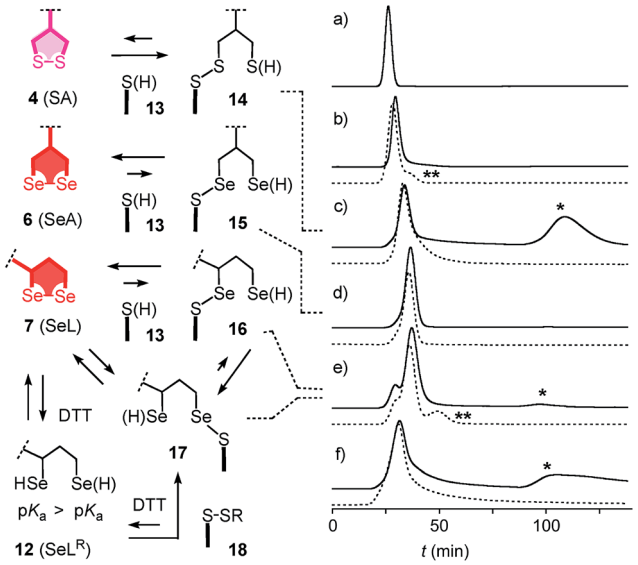

Fig. 3 Thiol-exchange affinity chromatograms of (a) CF, (b) ETP **5**, (c) SA **4**, (d) SeA **6**, (e) SeL **7** and (f) SeC **1** in 10 mM Tris, 0.1 M NaCl, 1 mM EDTA, pH 7.5 with a 0–50 mM DTT gradient at t = 60–70 min (solid) and constant 50 mM DTT from t = 0 (dashed). * = peaks indicative for inert binding of **1**, **4** and **7** to thiols on the stationary phase by strain-releasing thiol-disulfide/diselenide exchange in the absence of DTT. ** = peaks indicative for labile binding of reduced forms (*e.g.* SeL^R **12**) to disulfides on the stationary phase by thiol/selenol–disulfide exchange in the presence of DTT. Structures are shown in neutral form, acidic protons are indicated in parenthesis.

for temporal covalent bonding with the solid phase through thiol exchange (Fig. 3b–f, solid). Although the retention time of these peaks was shortened a little (~1 min) in the presence of DTT in the mobile phase (Fig. 3b–f, dashed), these retentions supported but did not prove transient dynamic covalent binding to the solid phase.

With SA **4**, a second broad peak eluted only upon addition of DTT to the mobile phase (Fig. 3c, *). This observation confirmed the formation and stability of the ring-opened, strain-released exchange product **14** by covalent attachment to the stationary phase. The absence of this second peak with SeA **6** indicated that ring-opened S–Se product **15**, if formed on the exchange column, ring closes rapidly back to SeA **6** (Fig. 3d). This result was consistent with expectations from the reduced ring tension in 1,2-diselenolanes compared to 1,2-dithiolanes, selenophilicity and the low pK_a of the selenol (Fig. 1). The importance of this low pK_a was confirmed by the absence of this second DTT-dependent peak also for ETP **5** with thiols of comparable acidity (Fig. 1 and 3b).

With SeL **7**, a second broad peak could be observed upon addition of DTT to the mobile phase (Fig. 3e, *). This finding provided direct experimental evidence for the occurrence of thiol-diselenide exchange with SeL **7**, *i.e.*, existence of the ring-opened S–Se product **16**. This S–Se product **16** and not the constitutional isomer **17** was presumably formed first because a primary selenolate with a lower pK_a is a better leaving group than the secondary selenolate with a higher pK_a. However, S–Se isomer **16** was expected to exchange intramolecularly because the secondary selenol in S–Se isomer **17** with a higher pK_a is a weaker nucleophile. The reduced reactivity of this S–Se isomer **17** with a secondary selenol could explain the detectability of the second, DTT-dependent peak in the affinity chromatogram of SeL **7** but not for SA **6** with primary selenols only (Fig. 3e, *). The isomerization from more reactive **16** to less reactive **17** could also account for the split of the first-eluting peak into two, a behavior that was unique for SeL **7** (Fig. 3e). An intense, very broad, DTT-dependent second peak was also observed with the acyclic diseleno cystine SeC **1** (Fig. 1 and 3f, *). The appearance of this peak was as expected because of the absence of a nearby selenol for rapid release by intramolecular exchange.

In the permanent presence of 50 mM DTT in the mobile phase, the fast eluting double peak of SeL **7** at R_t = 36.1 min was followed by smaller but significant additional peak (Fig. 3e, **). A similar peak occurred also with ETP **5** (Fig. 3b, **). A possible explanation of this observation was that DTT reduces SeL **7** to the diselenol **12** (Fig. 2), which then offers the activated primary selenolate to exchange with "hidden" disulfides **18** on the solid phase to give the more stable selenosulfide **17**, which undergoes ring closure or exchanges with DTT slowly enough to appear as separate peak. The same arguments were applicable to ETP **5**. This plausible explanation implied the existence of less reactive disulfides **18** on the solid phase that resist DTT but not the more reactive SeL^R **12** and reduced ETP **5**. Although speculative, this conclusion caught our full attention because it would be consistent with unique properties of SeL **7** and ETP **5** with regard to cellular uptake (see below).

Further support of the possible thiol-diselenide exchange was obtained by measuring the oxidation kinetics of DTT **19** to DTT^O **20** catalyzed by diselenides.[15] In the presence of one equivalent seleno lipoic acid **9**, the halflife time of DTT **19** decreased from t_{50} ≈ 16 h (Fig. 4, ○) to t_{50} ≈ 6.9 h (Fig. 4, ■). This rate enhancement confirmed the occurrence of thiol/diselenide exchange, the existence of intermediate **21** with mixed S–Se bonds and fast oxidation of SeL^R **12′** by molecular oxygen. The catalysis of DTT oxidation by 1,2-diselenolane **9** also demonstrated that the reloading of ring tension in **9** is less

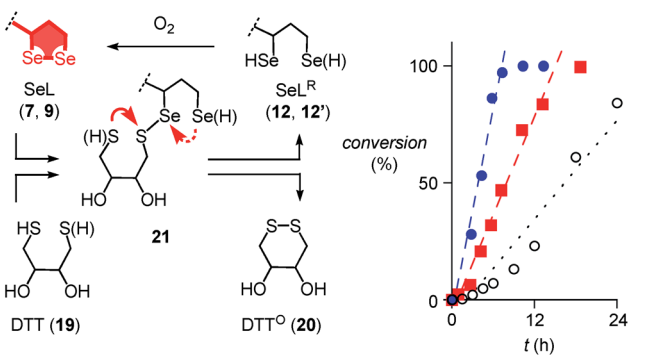

Fig. 4 Oxidation of 500 μM **19** to **20** as a function of time in the absence (○) and the presence of 500 μM **9** (■) and **22** (●) in D_2O, pD = 8.0, with linear fits to determine the t_{50}. Structures are shown in neutral form, acidic protons are indicated in parenthesis. Competing ring closures in reactive intermediate **21** are indicated with solid (preferred) and dashed red arrows.

favored than ring closure of DTT into the much less strained DTT^{O} **20** (Fig. 4, arrows).

Even more significant rate enhancements for DTT oxidation were observed with seleno asparagusic acid (SeA **22**, Fig. 2 and 4, ●). Compared to 1,2-diselenolane **9**, DTT lifetimes dropped further from $t_{50} \approx 6.9$ h to $t_{50} \approx 3.9$ h in the presence of SeA, and the final second-order rate constant increased from $k \approx 1.4 \times 10^{-2}$ M^{-1} s^{-1} to $k \approx 8.9 \times 10^{-2}$ M^{-1} s^{-1}. These results provided the experimental evidence for thiol-diselenide exchange for SeA that could not be secured unambiguously by thiol-exchange affinity chromatography (Fig. 3d).

In summary, the passage through thiol-exchange affinity columns complemented by DTT oxidation catalysis reflected pertinent aspects of cellular uptake well (see below).[1,2] The results demonstrated compatibility of 1,2-diselenolanes with strain-promoted thiol-mediated uptake. Moreover, evidence became available for dynamic covalent exchange with thiols on the cell surface, possible hopping along thiols or disulfides, facile intracellular release, possible participation of less reactive cellular disulfides and thiols, and clear differences between diselenides SeL **7**, SeA **6** and SeC **1** as well as disulfides SA **4** and ETP **5**.

The quantitative detection of cellular uptake was complicated by the fluorescence quenching with 1,2-diselenolanes. Compared to already strongly quenched 1,2-dithiolane SA **4**, 1,2-diselenolanes SeL **7** and SeA **6** displayed even weaker emission of FITC in buffer by factors of 4.6 and 3.3, respectively (Fig. 5b, solid, blue, red *vs.* green). Adding the 3.4-fold quenching of free FITC by 1,2-dithiolane in **4**,[1] the total quenching by 1,2-diselenolane calculated to a factor of up to 15.6. Fluorescence partially recovered upon reduction with TCEP (Fig. 2, 5a and b). Compared to reduced SA **4**, correction factors of 1.9 and 1.5 were obtained for SeL^{R} **12** and reduced form of SeA **6** (Fig. 5b, dashed, blue, red *vs.* green). For the quantification of uptake experiments, correction factors for closed cycles were applied.

The uptake of the green-fluorescent SA **4**, SeA **6** and SeL **7** into HeLa Kyoto cells was monitored by flow cytometry and confocal laser scanning microscopy (CLSM). Flow cytometry analysis with 10 μM of diselenides in Leibovitz medium at 37 °C showed a gradually increasing uptake with time, with 1,2-diselenolanes being much more active than 1,2-dithiolane SA **4**, and with SeL **7** outperforming SeA **6** (Fig. 5c).

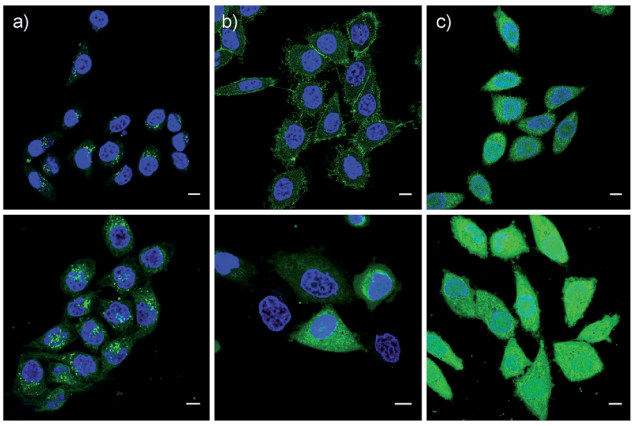

Fig. 6 CLSM images of HeLa Kyoto cells after 1 h of incubation with 50 μM (top) and 100 μM (bottom) SA **4** (a), SeA **6** (b) and SeL **7** (c) in Leibovitz medium at 37 °C, together with Hoechst 33342 to stain the nuclei (blue). Scale bar = 10 μm. LP = 0.8% for CF and 6.5% for Hoechst.

These impressions were confirmed in CLSM images, taken after one hour of incubation. Dithiolane SA **4** showed the known punctate emission characteristic for substantial capture in endosomes, together with significant homogeneous emission from the cytosol (Fig. 6a). SeA **6** showed stronger and more homogeneous emission at 50 μM but was visibly cytotoxic at 100 μM (Fig. 6b). With SeL **7**, intact cells were stained brightly and homogeneously including nuclei, at 50 μM and also at 100 μM (Fig. 6c).

Cytotoxicity was determined with the MTT assay, an assay that reports on the metabolic activity of the cells. Like SA **4** and ETP **5**, SeL **7** was not cytotoxic up to concentrations as high as 100 μM (Fig. 7a). As indicated by CLSM images (Fig. 6b), cytotoxicity started to emerge at 100 μM of SeA **6**, although

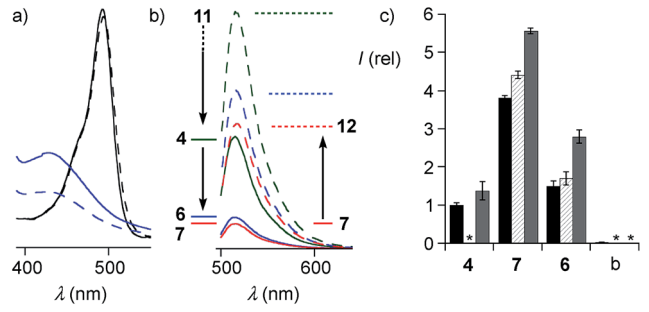

Fig. 5 (a) Absorption spectra of the isolated motifs FITC (black) and SeA (**22**, blue) before (solid) and after treatment with TCEP (dashed). (b) FITC emission from conjugates SA **4** (green), SeA **6** (blue) and SeL **7** (red, 100 μM, PBS) before (solid) and after (dashed) reduction with TCEP. (c) Flow cytometry results (mean ± error of three independent measurements) for uptake of 10 μM SA **4**, SeA **6** and SeL **7** and untreated (blank, b) HeLa Kyoto cells after incubation for 1 h (black), 2 h (hashed) and 4 h (grey), corrected for emission in closed form (b, solid). *Not determined.

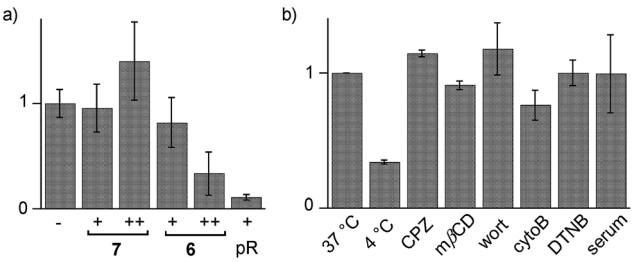

Fig. 7 (a) Cell viability from MTT assay with 0 ((−) normalized to 1.0), 10 (+) and 100 μM (++) of SeL **7**, SeA **6** or polyarginine (pR) in HeLa cells. (b) Flow cytometry data for HeLa Kyoto cells that were incubated with 10 μM SeL **7** at 37 °C (normalized to 1.0) and 4 °C, and cells that were preincubated with inhibitors of endocytosis (CPZ, mβCD, wort, cytoB) and thiol-mediated uptake (DTNB, 1.2 mM), followed by incubation with **7** at 37 °C, and incubation with 10% serum at 37 °C. Shown are average values ± error from three independent measurements.

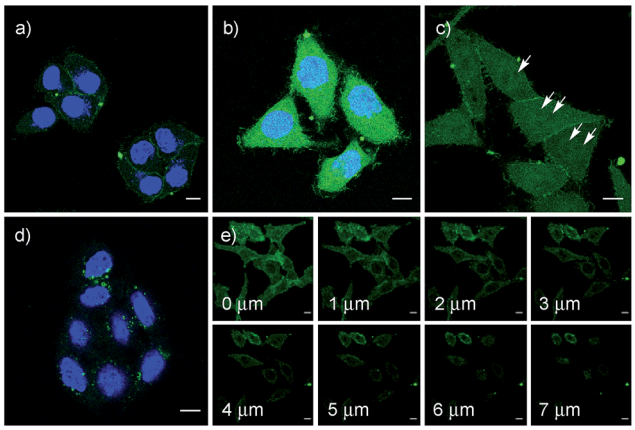

Fig. 8 CLSM images of HeLa Kyoto cells after incubation with 10 µM SeL **7** for 1 h (a), 2 h (b) and 4 h (c) (arrows indicate selected nucleoli), z-stacks ((e) 4 h, distances in *z*-axis) and 10 µM SeC **1** (4 h (d)); (a), (b) and (d) together with Hoechst 33342, blue. Scale bar = 10 µm. LP = 0.8% for CF and 6.5% for Hoechst.

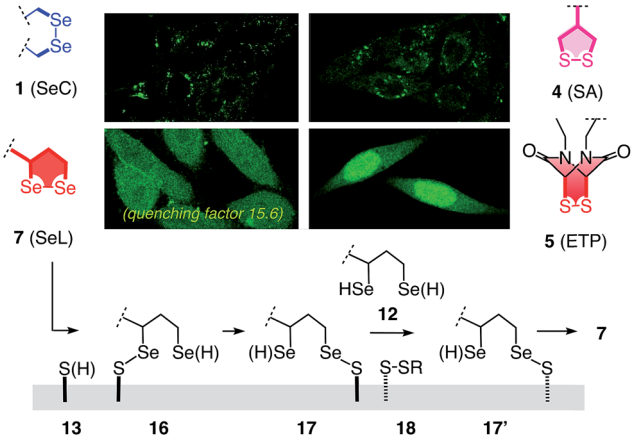

Fig. 9 Comparative summary of intracellular location of SeC **1**, SA **4**, ETP **5**,[2] and SeL **7**, and a tentative uptake mechanism for SeL **7**.

10 µM CPPs remained clearly more toxic (Fig. 7a). Studies on SeA **6** were thus discontinued.

Diselenolane-mediated uptake of SeL **7** was less sensitive to temperature than ETP-mediated uptake,[2] for instance (Fig. 7b). Insensitivity toward inhibitors supported that SeL does not enter cells by clathrin-mediated endocytosis (chlorpromazine; CPZ), caveolae-mediated endocytosis (methyl-β-cyclodextrin; mβCD) and macropinocytosis (wortmannin; wort, cytochalasin B; cytoB).[5] The presence of 10% serum slightly decelerated uptake without reducing final efficiency significantly. As for ETP **5** but neither for SA **4** nor SL **3**, uptake of SeL **7** was insensitive to DTNB, an inhibitor of conventional thiol-mediated uptake. In agreement with results from thiol-exchange affinity columns (Fig. 3), this might suggest that SeL **7** and ETP **5** can exchange also with less reactive thiols on the cell surface that are beyond reach of Ellman's reagent.

After longer incubation times, SeL **7** was efficiently delivered also at 10 µM (Fig. 8a–c). Z-stacks for SeL **7** confirmed that the homogeneous emission originates from cytosol (Fig. 8e). Corroborative support for delivery to cytosol and nucleus could be seen by the poor emission from nucleoli (Fig. 8d, arrows). Entry into the nucleus but not the nucleoli contrasted nicely to CPDs and other polycationic carriers that can accumulate in nucleoli, presumably due to interactions with polyanionic DNA,[5] and to ETP **5**, which targets the nucleus including nucleoli.[2]

The acyclic diseleno cystine SeC **1** showed weaker activity and mostly produced the punctate emission characteristic for endosomal capture (Fig. 8d and 9). This behavior was similar to SA **4** (Fig. 9) and in excellent agreement with mechanistic expectations from thiol exchange affinity columns (Fig. 3). More specifically, the selenosulfides obtained by thiol-diselenide exchange of SeC **1** on the cell surface are much more stable than with SeL **7** because the proximal covalent selenol for ring closure and release is missing (Fig. 3f *vs.* Fig. 3e). Uptake of this covalently attached selenosulfide could then occur by endocytosis and result in mostly endosomal capture, exactly as with SA **4** (Fig. 3f *vs.* 3c and 9).[6a] It is understood that SeC **1** is not a perfect acyclic mimic of SeL **7** because it contains an additional fluorophore. However, this difference was expected to be irrelevant with regard to the uptake mechanism under investigation, the second fluorophore released at the cell surface should be simply washed away before imaging. The agreement between mechanistic expectations and observed results in cells and on thiol-exchange columns supported that these assumptions are correct and SeC **1** and SeL **7** properly reveal the intrinsic differences between cellular uptake of acyclic and strained cyclic diselenides. Given the demonstrated usefulness of SA **4** to deliver peptides, liposomes and polymersomes also to the cytosol along this route,[6] this implied that delivery mediated by acyclic SeC **1** could be of substantial practical interest.

The clear difference of SA **4** and SeC **1** compared to ETP **5** and SeL **7** suggested that for dominant delivery to cytosol and nucleus with little endosomal capture, the release from covalent conjugates is essential (Fig. 9). The similar affinity chromatogram of the most active ETP **5** and SeL **7**, particularly the unique, DTT-dependent peak (Fig. 3, **), implied the transient existence of the fully reduced form and its exchange with less reactive cellular disulfides during uptake (**12**, Fig. 9). For 1,2-diselenolane-mediated uptake, this added up to a putative mechanism that begins with exchange of poorly reactive thiols **13** on the cell surface with SeL **7** (insensitivity to DTNB). The obtained selenosulfide **16**, covalently attached to the cell surface, rearranges to isomer **17** that is stable enough for detection by affinity chromatography (Fig. 3d*). Somewhere during uptake, thiol exchange with selenosulfide isomer **17** releases SeL^R **12**, which exchanges with less reactive cellular disulfides **18** before it can back-oxidize to **7** (interpretation of **peak in affinity chromatogram, Fig. 3). Further exchange with other cellular thiols **13** and disulfides **18** is possible until SeL **7** or SeL^R **12** are released into the cytosol (Fig. 4 and 9). The result for diselenolane-mediated cytosolic delivery with SeL **7** is a quite spectacular target hopping mechanism on different oxidation levels that will be extremely difficult to clarify in detail (Fig. 9).

The same conclusions apply to the similarly promising cytosolic delivery with ETP **5**.

Several possible additions and alternatives to this putative uptake mechanism exist. For instance, the free selenol next to the selenosulfide in conjugates **16** or **17** could exchange with another exofacial disulfide to produce a second selenosulfide and afford a more stable conjugate, whereas further dimerization of oligomerization are unlikely due to high dilution and fast ring closure (Fig. 9). Glutathione at the cell surface could be involved and possibly initiate uptake with partially or fully reduced SeL^{R} **12**, exchanging first with exofacial disulfides **18**, instead of oxidized SeL **7**, exchanging first with exofacial thiols **13** (Fig. 9).[3p,3q] Intracellular retention could contribute to uptake efficiencies and should influence intracellular location[21] (uptake of underivatized CF was negligible under experimental conditions[1,21]). These and other uncertainties concerning a complex mode of action should not distract from the key facts disclosed in this report: (a) Cytosolic delivery by SeL **7** is outstanding (Fig. 9).[22] (b) Clear differences to SeA **6** (cytotoxic, Fig. 6b and 7a; insensitive to affinity columns, Fig. 3d and e) indicate that a secondary selenol is essential (they very well reflect the distinct differences between SL and SA with regard to cellular uptake[1] and polymerization on surfaces[23] and in solution[24]). (c) Clear differences to SeC **1** (endosomal capture, Fig. 9; permanent retention on affinity columns, Fig. 3f and e) indicate that a strained cyclic diselenide is essential. (d) All trends, covering diselenides and disulfides from molecular modeling to affinity chromatography and intracellular localization, are consistent with conceptual expectations.

In summary, the move from sulfur to selenium affords the best carriers identified in this series so far. Cellular uptake mediated by 1,2-diselenolane **7**, *i.e.*, diseleno lipoic acid SeL, exceeds the performance of the best 1,2-dithiolane, *i.e.* SA **4** as well as the best disulfide at maximal ring tension, *i.e.* ETP **5**, with regard to both efficiency and intracellular localization. No trace of endosomal capture as with 1,2-dithiolane **4**, no trace of escape into the nucleus as with ETP **5**: diselenolane **7** delivers mostly to the cytosol (Fig. 9). The fluorescence images are particularly impressive with the strong quenching exerted by 1,2-diselenolanes taken into consideration (Fig. 5). The homologous 1,2-dithiolane SL **3** is clearly less performing not only than SeL **7** but also SA **4**.[1]

A comprehensive analysis of the nature of 1,2-diselenolanes compared to 1,2-dithiolanes reveals a combination of ring-tension, selenophilicity and the high but different acidity of primary and secondary selenols as the origin of the superb performance of 1,2-diselenolane **7**. Most importantly, thiol-exchange affinity chromatography is introduced to mimic and rationalize insights on thiol-mediated cellular uptake. The similar characteristics of ETP **5** and SeL **7** recorded by this method point toward an intriguing multitarget thiol hopping mechanism along so far unexplored routes to account for the efficient cytosolic delivery of these most powerful systems.[22,25]

Conflicts of interest

There are no conflicts of interest to declare.

Acknowledgements

We thank Xavier Martin-Benlloch for contributions to synthesis, the Roux group for assistance with cell culture, the NMR, the MS 2.0 and the Bioimaging Platform for services, and the University of Geneva, the Swiss National Centre of Competence in Research (NCCR) Chemical Biology, the NCCR Molecular Systems Engineering and the Swiss NSF for financial support.

Notes and references

1 G. Gasparini, G. Sargsyan, E.-K. Bang, N. Sakai and S. Matile, *Angew. Chem., Int. Ed.*, 2015, **54**, 7328–7331.
2 L. Zong, E. Bartolami, D. Abegg, A. Adibekian, N. Sakai and S. Matile, *ACS Cent. Sci.*, 2017, **3**, 449–453.
3 (*a*) S. Aubry, F. Burlina, E. Dupont, D. Delaroche, A. Juliot, S. Laveille, G. Chassaing and S. Sagan, *FASEB J.*, 2009, **23**, 2956–2967; (*b*) D. Oupický and J. Li, *Macromol. Biosci.*, 2014, **14**, 908–922; (*c*) Y. Y. Ling, J. Ren, T. Li, Y. B. Zhao and C. L. Wu, *Chem. Commun.*, 2016, **52**, 4533–4536; (*d*) J. Fu, C. Yu, L. Lu and S. Q. Yao, *J. Am. Chem. Soc.*, 2015, **137**, 12153–12160; (*e*) P. Yuan, H. Zhang, L. Qian, X. Mao, S. Du, C. Yu, B. Peng and S. Q. Yao, *Angew. Chem., Int. Ed.*, 2017, **56**, 12481–12485; (*f*) A. G. Torres and M. J. Gait, *Trends Biotechnol.*, 2012, **30**, 185–190; (*g*) L. Brülisauer, N. Kathriner, M. Prenrecaj, M. A. Gauthier and J.-C. Leroux, *Angew. Chem., Int. Ed.*, 2012, **51**, 12454–12458; (*h*) A. Kichler, J. S. Remy, O. Boussif, B. Frisch, C. Boeckler, J.-P. Behr and F. Schuber, *Biochem. Biophys. Res. Commun.*, 1995, **209**, 444–450; (*i*) E. P. Feener, W. C. Shen and H. J. P. Ryser, *J. Biol. Chem.*, 1990, **265**, 18780–18785; (*j*) P. K. Hashim, K. Okuro, S. Sasaki, Y. Hoashi and T. Aida, *J. Am. Chem. Soc.*, 2015, **137**, 15608–15611; (*k*) S. A. Bode, R. Wallbrecher, R. Brock, J. C. M. van Hest and D. W. P. M. Löwik, *Chem. Commun.*, 2014, **50**, 415–417; (*l*) C. R. Drake, A. Aissaoui, O. Argyros, M. Thanou, J. H. G. Steinke and A. D. Miller, *J. Controlled Release*, 2013, **171**, 81–90; (*m*) S. Son, R. Namgung, J. Kim, K. Singha and J. W. Kim, *Acc. Chem. Res.*, 2012, **45**, 1100–1112; (*n*) T.-I. Kim and S. W. Kim, *React. Funct. Polym.*, 2011, **71**, 344–349; (*o*) M. Balakirev, G. Schoehn and J. Chroboczek, *Chem. Biol.*, 2000, **7**, 813–819; (*p*) W. Gao, T. Li, J. Wang, Y. Zhao and C. Wu, *Anal. Chem.*, 2017, **89**, 937–944; (*q*) T. Li, W. Gao, J. Liang, M. Zha, Y. Chen, Y. Zhao and C. Wu, *Anal. Chem.*, 2017, **89**, 8501–8508; (*r*) D. Jha, R. Mishra, S. Gottschalk, K.-H. Wiesmüller, K. Ugurbil, M. E. Maier and J. Engelmann, *Bioconjugate Chem.*, 2011, **22**, 319–328; (*s*) A. N. Shirazo, N. Salem El-Sayed, D. Mandal, R. K. Tiwari, K. Tavakoli, M. Etesham and K. Parang, *Bioorg. Med. Chem. Lett.*, 2016, **26**, 656–661.
4 T. Li and S. Takeoka, *Int. J. Nanomed.*, 2014, **9**, 2849–2861.
5 (*a*) G. Gasparini, E.-K. Bang, G. Molinard, D. V. Tulumello, S. Ward, S. O. Kelley, A. Roux, N. Sakai and S. Matile, *J. Am. Chem. Soc.*, 2014, **136**, 6069–6074; (*b*) P. Morelli and S. Matile, *Helv. Chim. Acta*, 2017, **100**, e1600370; (*c*) E. Derivery, E. Bartolami, S. Matile and M. Gonzalez-Gaitan, *J. Am. Chem. Soc.*, 2017, **139**, 10172–10175.

6 (*a*) D. Abegg, G. Gasparini, D. G. Hoch, A. Shuster, E. Bartolami, S. Matile and A. Adibekian, *J. Am. Chem. Soc.*, 2017, **139**, 231–238; (*b*) N. Chuard, G. Gasparini, D. Moreau, S. Lörcher, C. Palivan, W. Meier, N. Sakai and S. Matile, *Angew. Chem., Int. Ed.*, 2017, **56**, 2947–2950.

7 (*a*) T. G. Back and P. W. Codding, *Can. J. Chem.*, 1983, **61**, 2749–2752; (*b*) O. Foss, K. Johnsen and T. Reistad, *Acta Chem. Scand.*, 1964, **18**, 2345–2354.

8 J. Hildebrandt, T. Niksch, R. Trautwein, N. Häfner, H. Görls, M.-C. Barth, M. Dürst, I. B. Runnebaum and W. Weigand, *Phosphorus, Sulfur Silicon Relat. Elem.*, 2017, **192**, 182–186.

9 T. Niksch, H. Görls, M. Friedrich, R. Oilunkaniemi, R. Laitinen and W. Weigand, *Eur. J. Inorg. Chem.*, 2010, 74–94.

10 (*a*) G. Bergson, G. Claeson and L. Schotte, *Acta Chem. Scand.*, 1962, **16**, 1159–1174; (*b*) G. Bergson and G. Claeson, *Acta Chem. Scand.*, 1961, **15**, 1611–1613.

11 (*a*) B. R. Beno, K.-S. Yeung, M. D. Bartberger, L. D. Pennington and N. A. Meanwell, *J. Med. Chem.*, 2015, **58**, 4383–4438; (*b*) S. Benz, J. López-Andarias, J. Mareda, N. Sakai and S. Matile, *Angew. Chem., Int. Ed.*, 2017, **56**, 812–815.

12 (*a*) B. Rasmussen, A. Sorensen, H. Gotfredsen and M. Pittelkow, *Chem. Commun.*, 2014, **50**, 3716–3718; (*b*) R. J. Hondal, S. M. Marino and V. N. Gladyshev, *Antioxid. Redox Signaling*, 2013, **18**, 1675–1689; (*c*) J. Sayers, R. J. Payne and N. Winssinger, *Chem. Sci.*, 2018, DOI: 10.1039/c7sc02736b.

13 D. Steinmann, T. Nauser and W. H. Koppenol, *J. Org. Chem.*, 2010, **75**, 6696–6699.

14 W. H. H. Guenther, *J. Org. Chem.*, 1967, **32**, 3931–3933.

15 (*a*) J. Beld, K. J. Woycechowsky and D. Hilvert, *Biochemistry*, 2007, **46**, 5382–5390; (*b*) J. Beld, K. J. Woycechowsky and D. Hilvert, *Biochemistry*, 2008, **47**, 6985–6987.

16 J. C. Lukesh, B. VanVeller and R. T. Raines, *Angew. Chem., Int. Ed.*, 2013, **52**, 12901–12904.

17 J. Liu and S. Rozovsky, *Antioxid. Redox Signaling*, 2015, **23**, 795–813.

18 (*a*) H. Xu, W. Cao and X. Zhang, *Acc. Chem. Res.*, 2013, **46**, 1647–1658; (*b*) D. Yue, G. Cheng, Y. He, Y. Nie, Q. Jiang, X. Cai and Z. Gu, *J. Mater. Chem. B*, 2014, **2**, 7210–7221; (*c*) Y. Wang, L. Zhu, Y. Wang, L. Li, Y. Lu, L. Shen and L. W. Zhang, *ACS Appl. Mater. Interfaces*, 2016, **8**, 35106–35113.

19 F. Xu, Z.-Z. Yang and S.-J. Zhang, *Phosphorus, Sulfur Silicon Relat. Elem.*, 2013, **188**, 1312–1319.

20 M. Haratake, S. Matsumoto, M. Ono and M. Nakayama, *Bioconjugate Chem.*, 2008, **19**, 1831–1839.

21 S. Izumi, Y. Urano, K. Hanaoka, T. Terai and T. Nagano, *J. Am. Chem. Soc.*, 2009, **131**, 10189–10200.

22 Preliminary results support that diselenolane-mediated uptake is compatible with the cytosolic delivery of proteins. Studies toward practical applications to deliver substrates of free choice, from DNA and RNA[22a] to proteins[5c] and fluorescent probes,[22b] are ongoing. (*a*) C. Gehin, J. Montenegro, E.-K. Bang, S. Takayama, H. Hirose, S. Futaki, A. Cajaraville, S. Matile and H. Riezman, *J. Am. Chem. Soc.*, 2013, **135**, 9295–9298; (*b*) Q. Verolet, M. Dal Molin, A. Colom, A. Roux, L. Guénée, N. Sakai and S. Matile, *Helv. Chim. Acta*, 2017, **100**, e1600328.

23 A. Carmine, Y. Domoto, N. Sakai and S. Matile, *Chem.–Eur. J.*, 2013, **19**, 11558–11563.

24 E.-K. Bang, G. Gasparini, G. Molinard, A. Roux, N. Sakai and S. Matile, *J. Am. Chem. Soc.*, 2013, **135**, 2088–2091.

25 A pioneering study on the delivery of acyclic selenosulfides appeared during the evaluation process of this manuscript: C. C. Tjin, K. D. Otley, T. D. Baguley, P. Kurup, J. Xu, A. C. Nairn, P. J. Lombroso and J. A. Ellman, *ACS Cent. Sci.*, 2017, **3**, 1322–1328.